ASSESSMENT OF DAM BATHYMETRY USING GIS AND GEOSTATISTICAL METHODS. CASE STUDY OF THE GHRIB DAM (ALGERIA)

Souhila BENKACI [1*], Boualem REMINI [1], Salah Eddine CHECHAM [1]

DOI: 10.21163/GT_2025.201.12

ABSTRACT

Assessing variations in water depth at a dam is highly beneficial for dam managers, as it enables more effective management of sluice gates and improves the planning and coordination of emptying and dredging operations. In this context, our study aims to analyze the spatial variability of water depth based on a sample of 44922 bathymetric survey data points measured at the Ghrib dam level. Initially, an exploratory analysis was performed, during which outliers were removed. Four semivariograms fitting models were then tested: Exponential, Spherical, Circular and Gaussian. Model performance was assessed using cross-validation tests, including mean error (ME), mean square error (MSE), root mean square error (RMSE), standardized mean error (MSE) and standardized root mean square error (RMSSE). The Gaussian model yielded the best results and was thus selected for interpolation using ordinary kriging. The resulting bathymetric map highlighted distinct classes representing estimated water depths within the Ghrib dam reservoir. The minimum water depth was estimated at approximately 18 meters, with a maximum of around 53 meters, which corresponds to the maximum water depth observed at the dam wall (near the dike). This bathymetric map serves as a valuable decision-making tool. However, while the kriging technique proved effective in this study, it would be advisable to generate multiple bathymetric maps using alternative interpolation methods, such as universal kriging, IDW, or spline, and to validate the most accurate map by comparing the results of these different approaches.

Key-words: *Bathymetry, GIS, Geostatistical analysis, Kriging, Semivariogram.*

1. INTRODUCTION

Dam siltation is a critical issue for managers worldwide, particularly in semiarid regions such as North Africa. This phenomenon, which has been extensively studied in several works (Hairan et al., 2023; Hallouz and Meddi, 2022; Remini and Mokeddem, 2018), results from the accumulation of sediments caused by soil erosion in watersheds and riverbank undercutting during floods. Moreover, it poses a significant challenge for dam managers, as it progressively reduces dams' adequate storage capacity and can obstruct sluice gates, thereby reducing the operational dam lifespan (Remini and Toumi, 2017). It also significantly threatens water quality, ecological stability and sustainable resource management (Rashid and Pandit, 2023). A precise assessment of sedimentation levels is imperative to accurately characterize the scale of this phenomenon and to develop effective management strategies. Bathymetric surveys represent a fundamental methodology in this context. These surveys involve measuring reservoir depths to estimate sediment accumulation, which is crucial for determining the reduction in reservoir capacity over time (Mekonnen et al., 2022; Endalew and Mulu, 2022). Additionally, they facilitate the creation of digital seabed models that illustrate depth distribution across the reservoir (Pike et al., 2019). These models support both basic and advanced analyses, including the development of predictive maps for various seabed and water column phenomena (Zhu et al., 2020; Biernacik et al., 2023). However, the quality and reliability of the collected data can be influenced by environmental conditions, water clarity, and bottom reflectivity. These factors introduce variability and randomness in bathymetric measurements (Kelvin Kang and Mohd Razali, 2021). Consequently, bathymetric survey data are often regarded as random variables

[1] *Department of Water Sciences and Environment, Laboratory for the Preservation and Protection of WaterResources, University of Saad Dahlab, Blida 1, Algeria. Corresponding author: (SB) benkaci_souhila@univ-blida.dz, (BR) remini1961@gmail.com; (SEC) sansinou74@gmail.com*

due to inherent fluctuations and inconsistencies in the collected information (Makar, 2023; Wróbel et al., 2023; Wilson et al., 2022). This data exhibits spatial correlation, which can be effectively captured through geostatistical methods (Santra and Adhikary, 2021). The basic approach involves identifying and quantifying the spatial structure of the variables of interest, followed by estimating these variables based on neighbouring values, whilst accounting for their spatial structure (Maliva, 2016). This process also aims to detect, analyze, quantify, and model the spatial covariance of observations, providing a deeper understanding of spatial relationships in the data (Mälicke, 2022). Integrating geostatistical methods into a GIS environment streamlines the tasks associated with numerical methods, thereby rendering complex geostatistical approaches more accessible and visually intuitive within GIS software (Deutsch, 2021). This integration enhances the efficiency and accuracy of spatial data analysis and modelling (Yoo, 2018) and is further boosted by recent advancements in computing technology (Triki et al., 2014). Geostatistics provides robust tools to characterize the spatial properties of natural phenomena (Isaaks and Srivastava, 1989), while GIS software complements these capabilities by incorporating spatial modeling functionalities through specialized extensions (Thomas, 2003). The Geostatistical Analyst extension in ArcGIS is a case in point, offering an exploratory spatial data analysis module that facilitates data visualisation and analysis using statistical techniques (ESRI, 2014). This extension provides a wide array of spatial modeling functions, enabling the detection of trends, identification of outliers, and the exploration of spatial correlations within the data (Johnston et al., 2001). Among the most commonly used geostatistical methods for spatial prediction, ordinary kriging stands out as one of the most popular and accurate techniques for interpolating spatially varying data (Rojimol et al., 2021). This method has been extensively applied across various fields of environmental science worldwide (Arétouyap et al., 2016; Gharbia et al., 2016). In the context of water resources management, ordinary kriging is regarded as an indispensable tool for interpolation and spatial estimation (Adhikary et al., 2015; Gupta et al., 2017). It has been effectively used to predict water quality indices at unobserved sites, enabling the precise mapping of spatial distributions (Khana et al., 2023), and to estimate rainfall at unmeasured locations, thereby enhancing the accuracy of hydrological modeling (Adhikary et al., 2016). Furthermore, it has proven instrumental in accurately predicting groundwater levels, reducing errors in numerical models, enhancing monitoring efforts, and producing precise maps of the potentiometric surface (Asadi and Adhikari, 2022). Accurate interpolation is also vital for compiling bathymetric maps in water depth studies (Ivan, 2021). Ordinary kriging has been used to generate such maps, outperforming 14 other interpolation methods in a comparative analysis of bathymetric survey data. The results revealed that ordinary kriging produced the most accurate predictions, with validation demonstrating the lowest root mean square error (RMSE) among the tested interpolators (Šiljeg et al., 2015). Its effectiveness was further confirmed through cross-validation, where eight statistical parameters were evaluated, establishing ordinary kriging as the most reliable geostatistical interpolation method for producing bathymetric maps (Šiljeg et al., 2016; Alcaras et al., 2020).

In this context, the ordinary kriging technique was used to produce a representative bathymetric map, enabling the determination of water depth at any point on the Ghrib dam's surface. This dam is considered one of the most silted in Algeria (Benkaci et al., 2018). Since its construction in 1939, its storage has significantly decreased due to sedimentation issues, decreasing from 280 hm^3 to 115.32 hm^3 in 2004, which corresponds to a sedimentation rate of 58.81% (ANBT, 2004). In 2006, the dam's embankment was raised by 4.5 meters, increasing its capacity to approximately 195.32 hm^3 (Le Blanc, 2006). According to bathymetric surveys carried out in 2019, the reservoir capacity was estimated at approximately 169.35 hm^3 at a normal water level of 432 meters (ANBT, 2018). Several variogram models were tested using the cross-validation method. ArcGIS software enabled the selection of various functions (Circular, Spherical, Exponential, Gaussian and Linear) to model the empirical semivariogram when applying the kriging tool (Ivan, 2021). The performance of the ordinary kriging interpolation was subsequently assessed through statistical indices such as the mean absolute error (MAE) and root mean square error (RMSE) (Khan et al., 2021). This research enhances the understanding of sedimentation dynamics in Algerian reservoirs while highlighting the effectiveness of integrating geostatistical methods with GIS tools to address environmental challenges.

2. STUDY AREA

The Cheliff Ghrib catchment (**Fig.1**) constitutes one of eleven sub-watersheds within the Upper and Middle Cheliff (Benkaci, 2020), which in turn are part of the larger Cheliff-Zahrez basin, covering more than 22% of northern Algeria's land area (ABH., 2004). The catchment is situated approximately 100 km south-west of Algiers, between 2°25’ and 3°45’ east longitude and between 35°45’ and 36°00’ north altitude, with an average altitude of 895 m (Mokhtari et al.,2023). The watershed of Ghrib is elongated in shape along the axis of the mainstream, draining an area of 1378.67 km^2 with an average altitude of 895 m (Benallal et al.,2024).

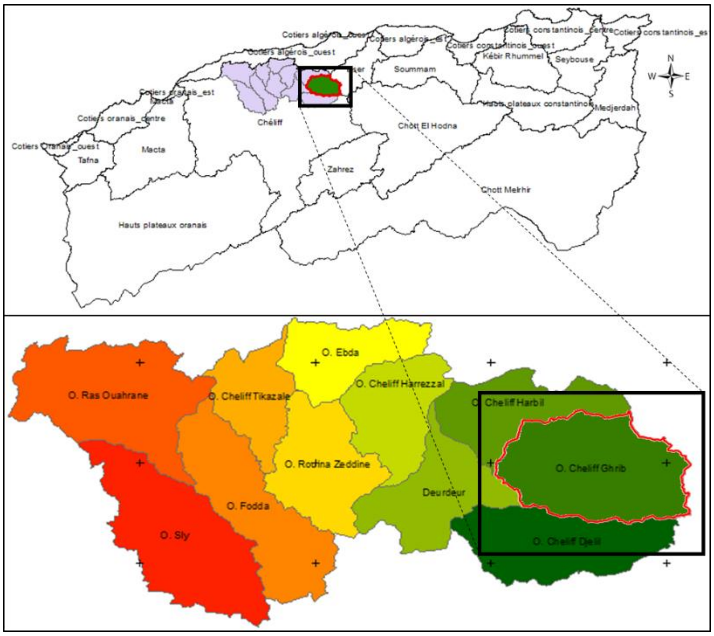

Fig. 1. Geographic location of the Cheliff-Ghrib sub-basin in Algeria.

The Ghrib sub-watershed is characterized by a strong and diverse relief (**Fig. 2**).

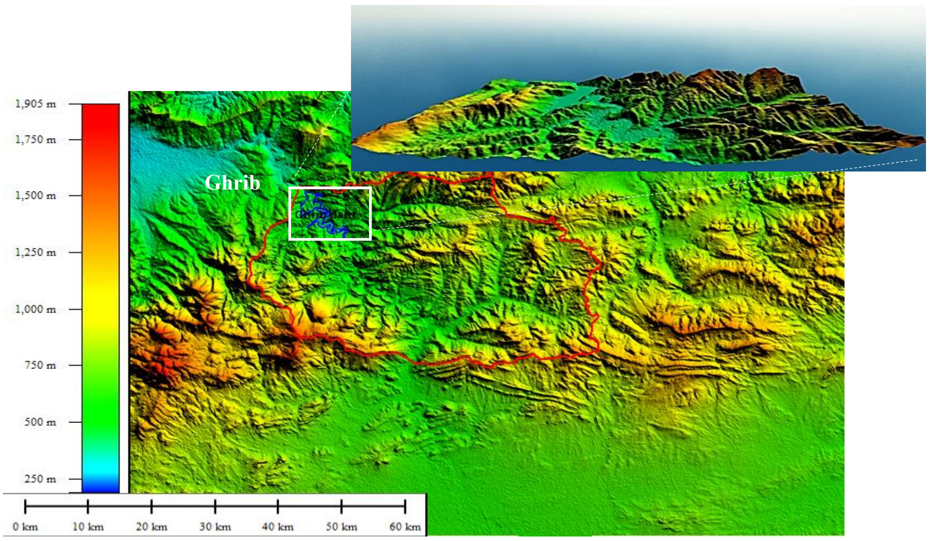

Fig. 2. Shuttle Radar Topography Mission (SRTM) image of the Cheliff-Ghrib sub-watershed.

In the southeastern region, mountains reach elevations of up to 1604 meters. In contrast, in the central part of the watershed features valleys with gentle slopes and relatively low altitudes, extending up to the dam. The Ghrib is a rockfill dam located on the Cheliff river, approximately 20 km southwest of the Ain-Defla city (Benkaci and Ghecham, 2021). It is part of the Cheliff-Ghrib sub-watershed and serves as a fundamental structure for the development of the Cheliff Valley. The dam is designed for irrigation, drinking water supply, and the transfer of water to the Bouroumi dam, with a regulated annual volume of 105 million cubic meters (ANBT, 2018). A reduced model of the Ghrib dam is depicted in **Fig. 3.**

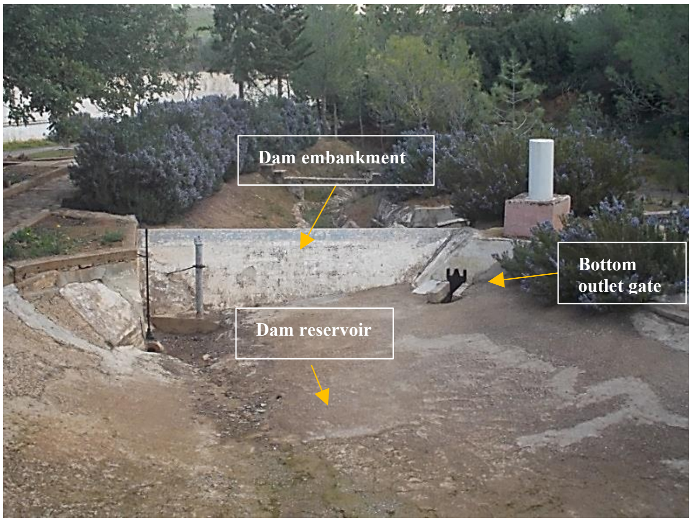

Fig. 3. Ghrib dam scale model 1:50 (Photo. Remini, 2019).

At the Ghrib dam reservoir, a significant increase in liquid inflows was observed, particularly during the years 2018-2019 (**Fig. 4**). In this period, the average annual capacity loss was estimated to be approximately 3.6 hm^3/year, based on the results of the most recent bathymetric surveys.

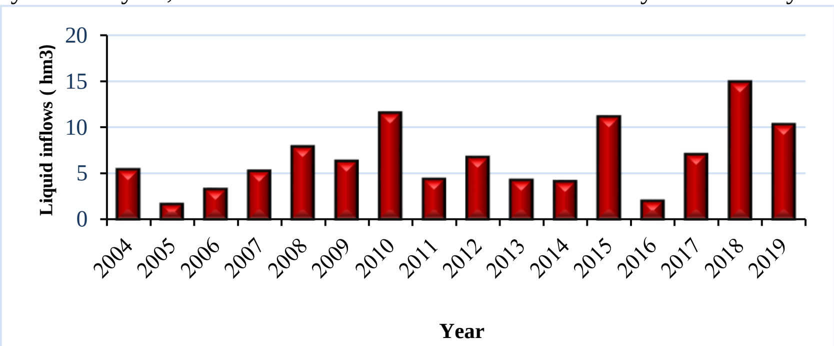

Fig. 4. Annual mean liquid inflows variation at the Ghrib Dam.

3. DATA AND METHODS

3.1. Bathymetric data

To achieve our objectives, we utilized the hydro-climatological network and water quality monitoring map for northern Algeria, produced by the National Institute of Cartography and Remote Sensing in Algiers. The map was digitized and georeferenced based on the Lambert conformal conic projection for the northern region of Algeria, and it was particularly useful for delimiting our study area (Benkaci, 2020). The spatial water depth variation within the Ghrib dam reservoir was analyzed based on bathymetric surveys, provided in Excel file format (with coordinates: latitude x, longitude y, and depth z). The data file was visualized using ArcGIS software, as shown in **Fig .5**

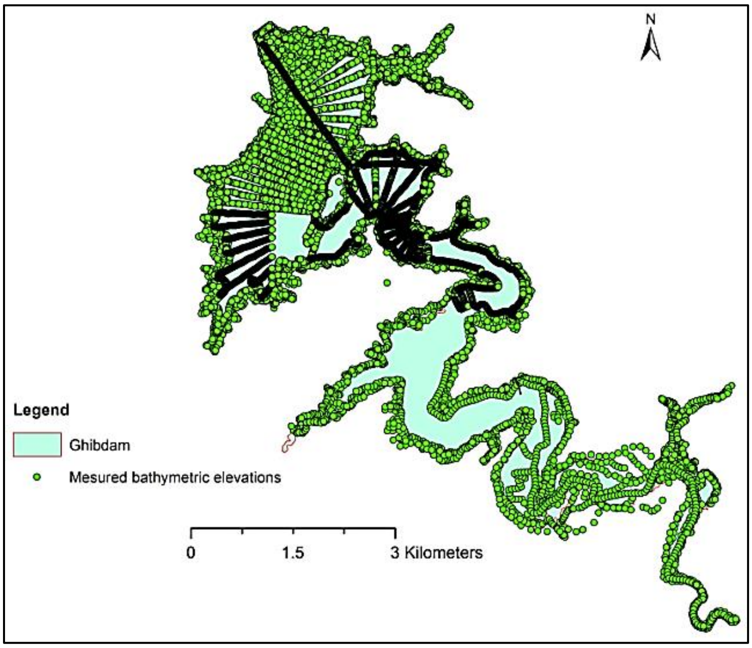

Fig. 5. Visualisation of bathymetric depths measured at the Ghrib dam in 2019.

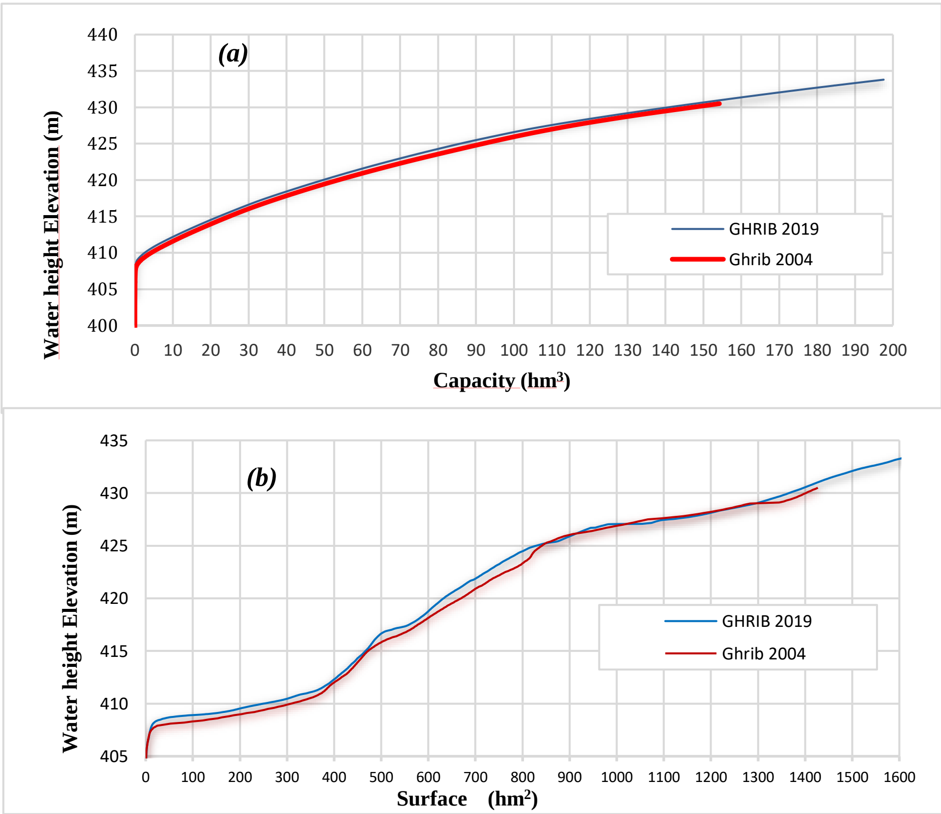

Fig. 6. Characteristics curve: (a) Height-capacity curve; (b) Height-Surface curve.

The Excel file of bathymetric data allowed us to plot height- capacity and height - surface curves (**Fig. 6**). These curves represent the water volume stored in the reservoir, accounting for accumulated sediment. They can be used for reservoir operation, flood routing, and determining capacity and discharge at different elevations (Tobgay, 2014). The stability of these curves over time is influenced by the accumulation of solid deposits within the reservoir. The general appearance of the curves depicted in the Figure 7 does not reveal any specific features related to relief irregularities. However, a proportional evolution of the storage surface and capacity of the Ghrib dam can be observed from 2004 to the most recent bathymetric surveys conducted in 2019.

3.2. Methodological Diagram

Various treatments were performed using the "Geostatistical Analysis" tool in ArcGIS, based on the assumption that the regionalized variable Z (depth) is a random variable defined as a numerical function Z(s), where "s" is a vector consisting of three components: latitude, longitude, and depth. The distribution of different values across the defined area follows a random phenomenon (Benkaci, 2020). The steps taken to complete our work are outlined in the methodological flowchart presented in **Fig. 7**

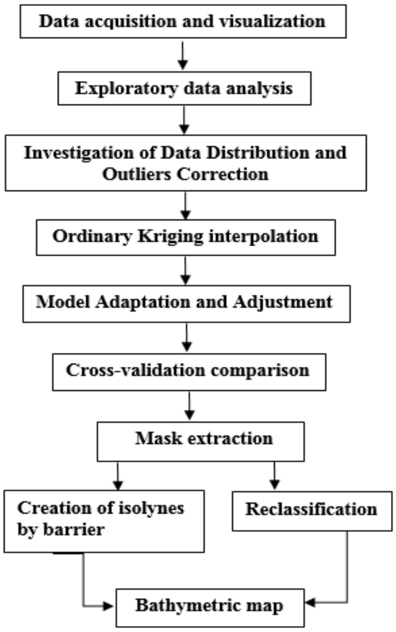

Fig. 7. Methodological Diagram.

3.3. Exploratory data analysis

The variables used correspond to the most recent bathymetric surveys conducted at the Ghrib dam reservoir. These data were obtained in the form of an Excel file containing 44922 values (after outliers were removed). The values were imported into ArcGIS software for visualization and were analyzed using the histogram tool (**Fig. 8**) and the normal QQ plot (**Fig. 9**) to assess their distribution pattern.

Table 1 provides a summary of the statistical information for the data. To ensure accurate geostatistical analysis, it is important to verify the values follow a normal distribution. This verification can be done by checking whether the mean and median values are similar, and whether the skewness, also known as Pearson’s moment coefficient, is close to zero (Gundogdu, 2015; Rigby et al., 2019).

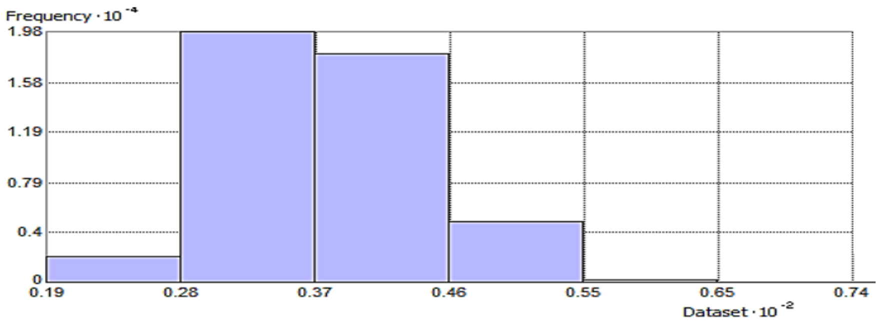

Fig. 8. Histogram of water depth distribution**.**

Table 1.

Experimental variogram modeling parameters.

Statistics	**Sampled bathymetry (m)**
Min value	18.59
Max value	110.73
Mean value	36.912
Std. Dev.	7.4405
Skewness	0.54331
Kurtosis	3.6738
1st Quartile	29.49
Median	37.28
3rd Quartile	41.45

Figure 9 displays a unimodal, asymmetrical histogram, indicating that the data does not follow a normal distribution. The skewness value of 0.54 and kurtosis value of 3.67 confirm the rightward asymmetry. Furthermore, Table 1 illustrates that 25% of the values fall below 29.49 meters, 25% exceed 41.45 meters, and 50% of the values are centered around an average of 37 meters. This average represents the water depth stored in the Ghrib dam reservoir in 2019. Additionally, a standard QQ-Plot allows us to compare the data against a normal distribution (Gundogdu, 2015).

The QQ plot diagram, shown in **Fig. 10**, reveals that the bathymetric values deviate from the straight line (Grekousis, 2020), indicating the presence of outliers.

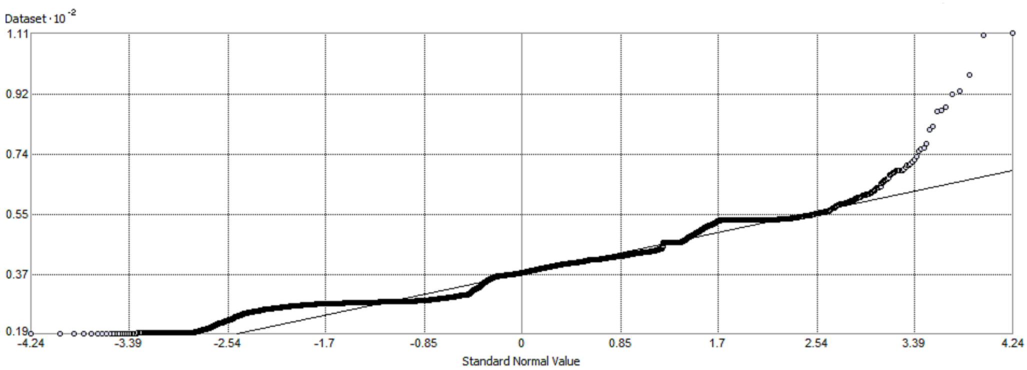

Fig. 9. QQ-Plot Diagram.

These variations in values may result from differences in the dam's bottom topography, such as the presence of obstacles, sediment accumulation, erosion caused by the opening or closing of the bottom gates, or other factors. The main advantage of using the attribute table derived from the QQ-plot is that it allowed us to correct the most outlying points that deviate from the line (**Fig. 10**). This step is crucial for selecting the appropriate interpolation method, particularly ordinary kriging.

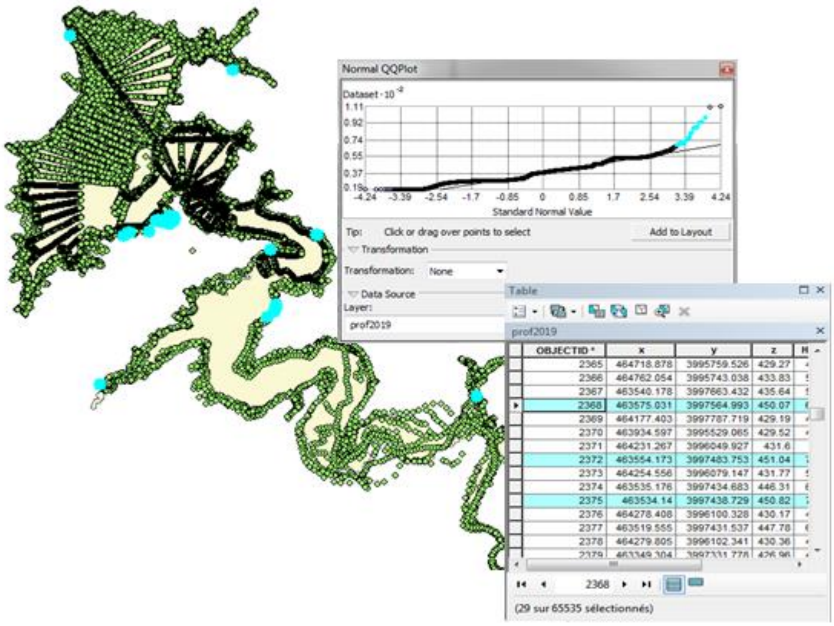

Fig. 10. Correction and removal of the outlier points.

Furthermore, the analysis depicted in **Fig. 11** facilitates the identification of patterns within the input dataset and the selection of the polynomial order that best represents each trend (Biernacik et al., 2023). The results reveal a decrease in bathymetric values (z) as the Y coordinate increases, following a south-to-north direction.

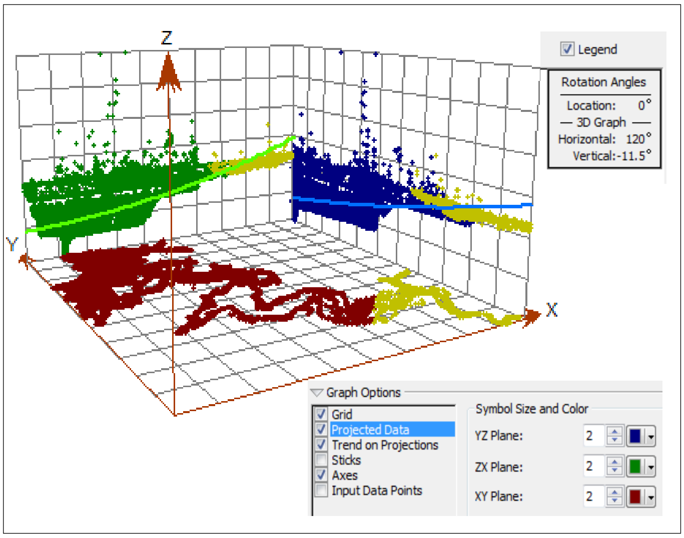

Fig. 11. Spatial trend of of the bathymetric variable.

The northern and western directions, corresponding to the dam reservoir center, exhibit a high point density, which gradually diminishes along the X direction (upstream of the reservoir). However, at the Cheliff River mouth, the values become more scattered, deviating significantly from the modeled lines and showing noticeably higher elevations. The final stage of the exploratory analysis involved examining the variogram, which shows the correlation cloud of quadratic deviations [z(si + h) - z(si)] as a distance function between the experimental points (Wieskotten, 2023; Desnoyers, 2010).

The variograms shown in **Fig. 12** were calculated for all combinations of the regionalized variable corresponding to the bathymetric data collected in the Ghrib dam area. It was observed that the point dataset exhibited significant discontinuities at short distances (0 - 230 m), regardless of the direction or tolerance angle, with many isolated points present. These outliers indicate abnormal samples (Triki, 2014; Cardenas, 2004). Their presence hinders adequate adjustment and complicates the variogram analysis. Consequently, the resulting variographic surface appeared entirely uniform across any selected distances and directions (Cardenas, 2004).

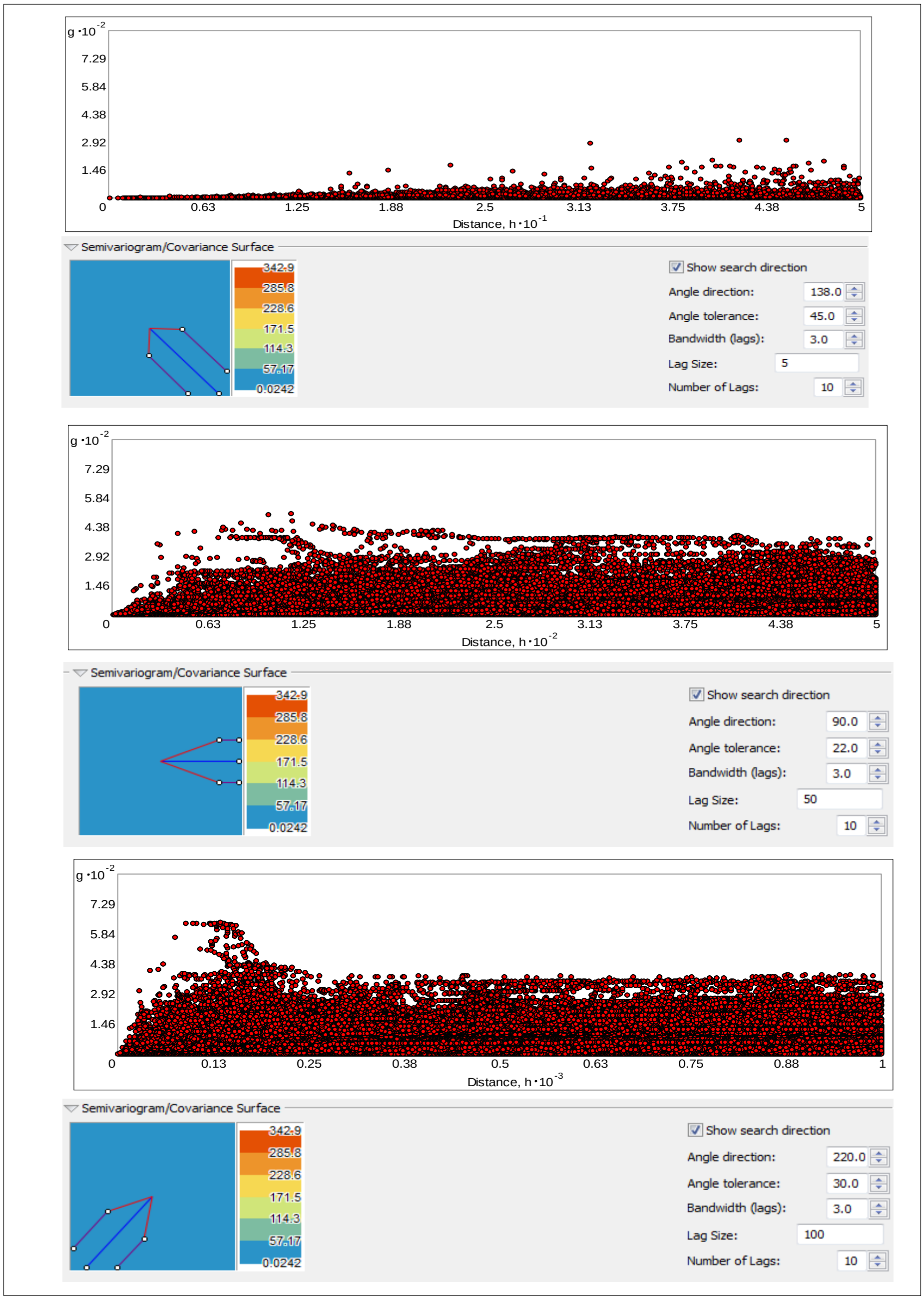

Fig. 12. Directional variogram and varigraphic surface for short distances.

At greater distances, up to 1.5 km, the variogram in **Fig. 13** highlights an anisotropic structure with strong spatial variability in the 138° direction, with a tolerance angle of 45 °. This direction approximately corresponds to the water flow direction from the Oued Cheliff to the Ghrib dam reservoir. This anisotropy can be attributed to the irregularities in the bathymetric depths, influenced by the uneven bottom morphology associated with erosion and sedimentation zones.

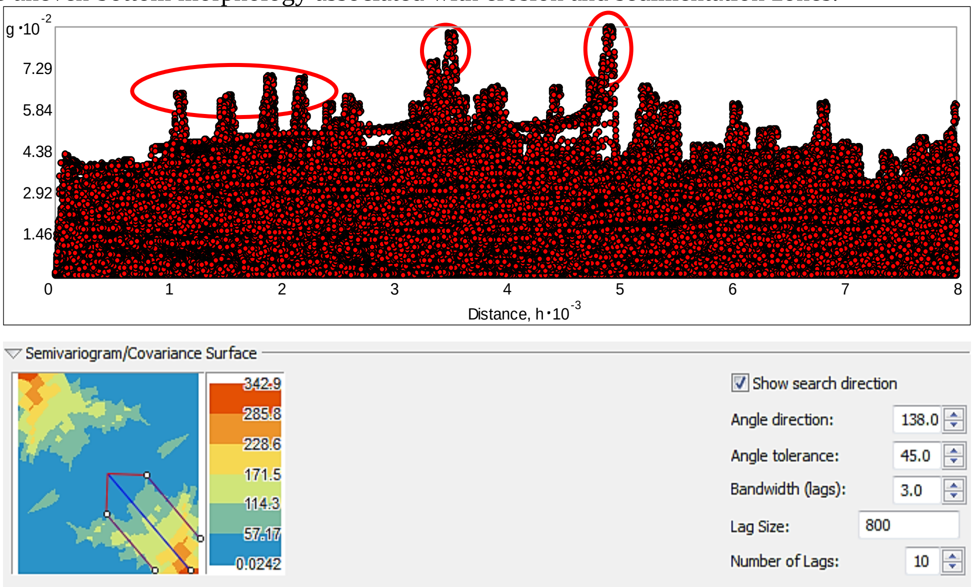

Fig. 13. Variogram and variographic surface.

The reddish circles in **Fig. 13** indicate significantly high semivariogram values for pairs of points that are in close proximity. These isolated values may be attributed to the high-elevation areas upstream of the Ghrib dam. However, a more detailed analysis is required to pinpoint the specific sources of these variations, which falls outside the scope of this study (Asadi and Adhikari, 2022).

3.4. Model adaptation and Adjustment

The fundamental geostatistical tool essential for implementing and selecting the interpolation model is the variogram (Meylan 1986). It is crucial for characterizing spatial autocorrelation in datasets (Seddiki and Dehimi 2023). The variogram is represented by an estimator γ (semivariogram) which is defined as follows (Chauvet 1992):

$$\gamma(h) = \frac{1}{2} var[Z(s) - Z(s+h)] = \frac{1}{2} E\left[\left(Z(s) - Z(s+h)\right)^2\right] \quad (1)$$

where:

$Z(s)$	-observed value at the location s;
$Z(s+h)$	-value of a point at lag h from location *s*;
$Var\,[Z(s+h) - Z(s)]$	-variance of the random variable $[Z(s+h) - Z(s)]$;
$E\left[\left(Z(s+h) - Z(s)\right)^2\right]$	-random variable's quadratic expectation;

As illustrated in **Fig. 14**, variographic parameters consist of the following elements (Mälicke, 2022 ; Khan et al., 2021; Seddiki and Dehimi, 2023 ; Mazzella, 2013) :

- **nugget effect (C_0)**: This represents the initial variability value, which is the variance that cannot be explained by a spatial model. It is depicted by the semi-variance at lag *h*=0.
- **range (C_0+C_1):** this is the distance (measured in units of the horizontal axis) beyond which the data become completely independent, meaning the correlation between observations becomes zero.

- **sill (C_0+C_1)** : corresponding to the total variance of a spatial dataset and is defined as the sum of the nugget effect (C_0) and the partial sill (C_1).

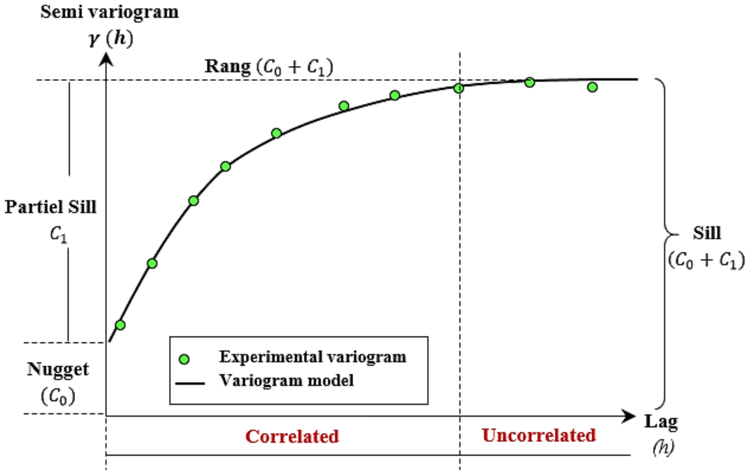

Fig. 14. Illustration of the variogram model parameters.

The theoretical variogram (Eq. (1)) is not explicitly defined; however, it can be estimated from the sample data. The experimental variogram can then be derived as follows (Seddiki and Dehimi, 2023; Malherbe and Rouïl, 2003; AbdelRahman at al.,.2021):

$$\hat{\gamma}(h) = \frac{1}{2N(h)} \sum_{N(h)} \left[z(s_i) - z(s_j)\right]^2 \tag{2}$$

where:

$N(h)$ - number of point pairs for the lag h;

$Z(s)$ - observed value at the respective location s;

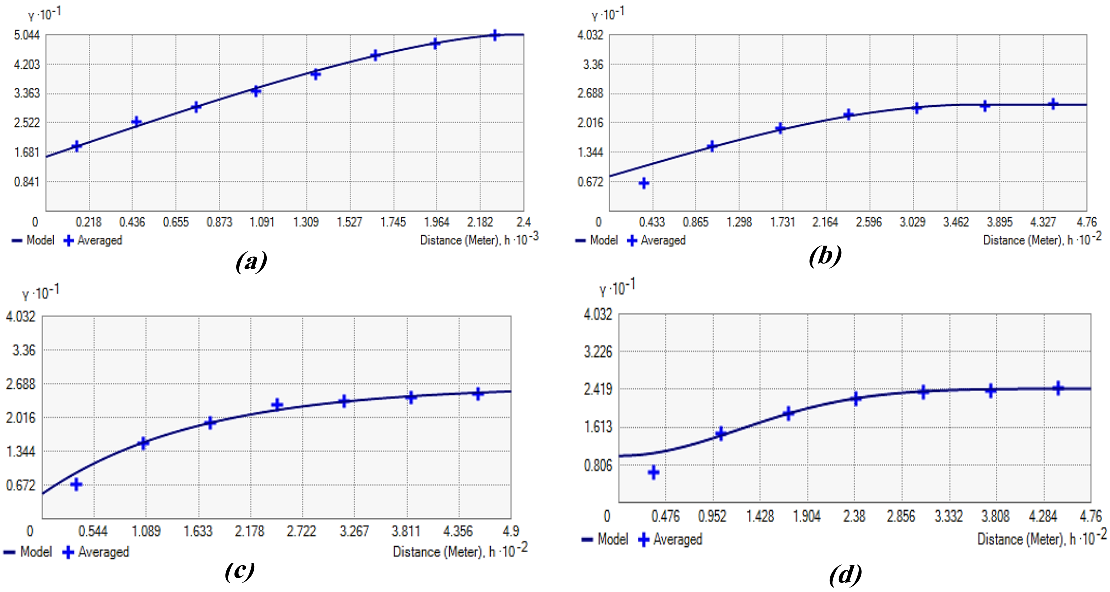

Fig. 15. Experimental Variograms: (a) Circular Model, (b) Spherical Model, (c) Exponential Model, (d) Gaussian Model.

The spatial variation of the Z(s) values corresponding to the bathymetry is quantified by studying the semivariogram, which involves fitting a theoretical variogram to the experimental variogram. Four of the most commonly used models were tested using ArcGIS software: Circular, Spherical, Exponential, and Gaussian. The results are presented in **Fig. 15**
The parameters of the four models fitted to these experimental variogram are illustrated in **Table 2**.

Table 2.

Experimental variogram modeling parameters.

Semi-variogram model	**Experimental Semi-variogram**		**Nugget**	**Range**	**Sill**
	Number of lags	Lag Size (m)			
Circular	08	300	15.57	2302.338	50.4319
Spherical	07	68	08.00	366.3397	24.37955
Exponential	07	70	05.00	490.0000	26.43355
Gaussian	07	100	10.00	297.4198	24.36696

For all four models, the variogram exhibits a discontinuity at the origin (nugget effect), indicating that the measured bathymetric values change abruptly over short distances. This local variability can be attributed to random phenomena, including undetectable measurement errors arising from the significant distance between observations (Arnaud and Emery, 2000). The semivariograms of the Exponential, Spherical, and Gaussian models demonstrate very similar ranges, with an average distance of 25 meters, suggesting that the variables are independent and that there is no correlation between the measurement points.

4. RESULTS AND DISCUSSIONS

4.1. Cross-validation comparison

Once the experimental variogram has been fitted to a model with specific parameters (nugget, range, etc.) (Arnaud and Emery 2000), the predictive performance of the provided models is evaluated through cross-validation (Boubaker et al., 2010; Seddiki and Dehimi, 2023; Selmy et al., 2022). This process assesses the suitability of the selected model using the experimental data and is necessary before generating the final interpolation surface (Biernacik et al., 2023). The principle involves temporarily omitting each observation in turn (using Kriging) and estimating its value based on the remaining neighboring data. The estimation error is then calculated at each data point and compared with the standard deviation of the estimates provided by Kriging (Arnaud and Emery, 2000). The four tested models were compared using cross-validation, and the results are presented in **Fig. 16**

The performance of the kriging interpolation was then evaluated using the following prediction errors: mean error (ME), mean standard error (MSE), root-mean-square error (RMSE), and root-mean-square standardized error (RMSSE) (Selmy et al., 2022; Alcaras et al., 2022; Qi et al., 2021; Varouchakis et al., 2022). These errors were calculated using equations (Eq. (3)), (Eq. (4)), (Eq. (5)) and (Eq. (6)), respectively:

$$ME = \frac{1}{N}\sum_{i=1}^{N}[z^*(s_i) - z(s_i)] \qquad (3)$$

$$MSE = \frac{1}{N}\sum_{i=1}^{N}\left[\frac{z^*(s_i) - z(s_i)}{\delta^2(s_i)}\right] \qquad (4)$$

$$RMSE = \sqrt{\frac{1}{N}\sum_{i=1}^{N}[z^*(s_i) - z(s_i)]^2} \qquad (5)$$

$$RMSSE = \sqrt{\frac{1}{N}\sum_{i=1}^{N}\frac{[z^*(s_i) - z(s_i)]^2}{\delta^2(s_i)}} \quad (6)$$

where:

$Z(s)$ -observed value at the respective location s;

Z*(si) -value predicted by the model at the same location;

N - number of samples;

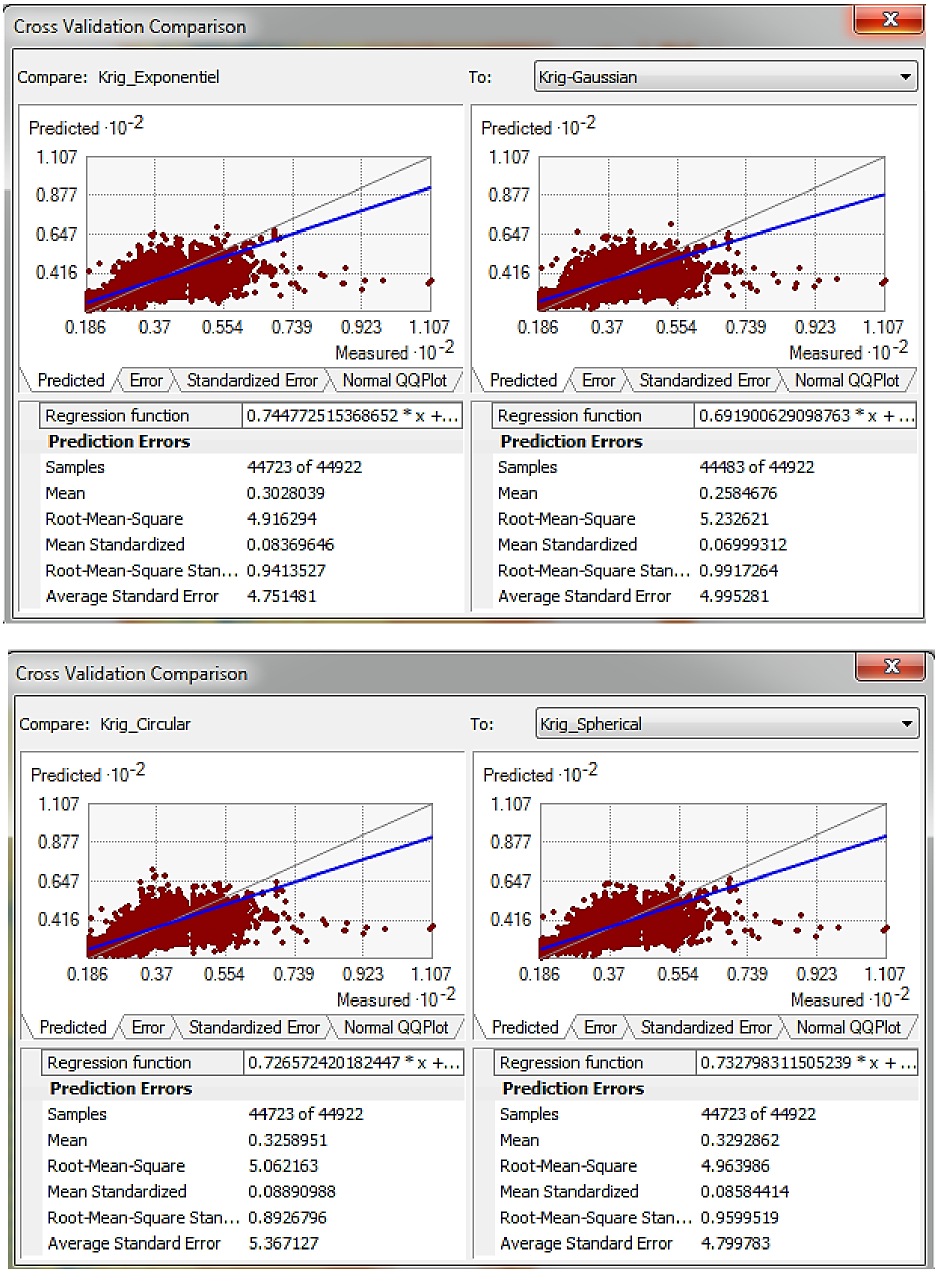

Fig. 16. Cross-validation comparison of the four models: (a) Gaussian and Exponential models, (b) Circular and Spherical models.

Table 3 indicates that the Gaussian model exhibits the best fit, as evidenced by the root-mean-square-standardized (RMSSE) being close to one, and the mean standardized of the estimation error (MSE) being the lowest and almost zero “0”. Therefore, the Gaussian model was chosen for the kriging interpolation to generate the bathymetry prediction map of the Ghrib dam reservoir.

Table 3.

Comparison of cross-validation results for the Four tested models.

Semivariogram model	Mean error (ME)	Root mean square (RMSE)	Mean standardized error (MSE)	Root mean square standard. (RMSSE)
Circular	0.3258951	5.062163	0.08890988	0. 8926796
Spherical	0.3292862	4.963986	0.08584414	0.9599519
Exponential	0.3028039	4.916294	0.08369646	0.9413527
Gaussian	0.2584676	5.232621	0.06999312	0.9917264

4.2. Bathymetric map creation

The bathymetric prediction map for the Ghrib dam reservoir was generated using ordinary Kriging interpolation based on the Gaussian model (**Fig.17**).

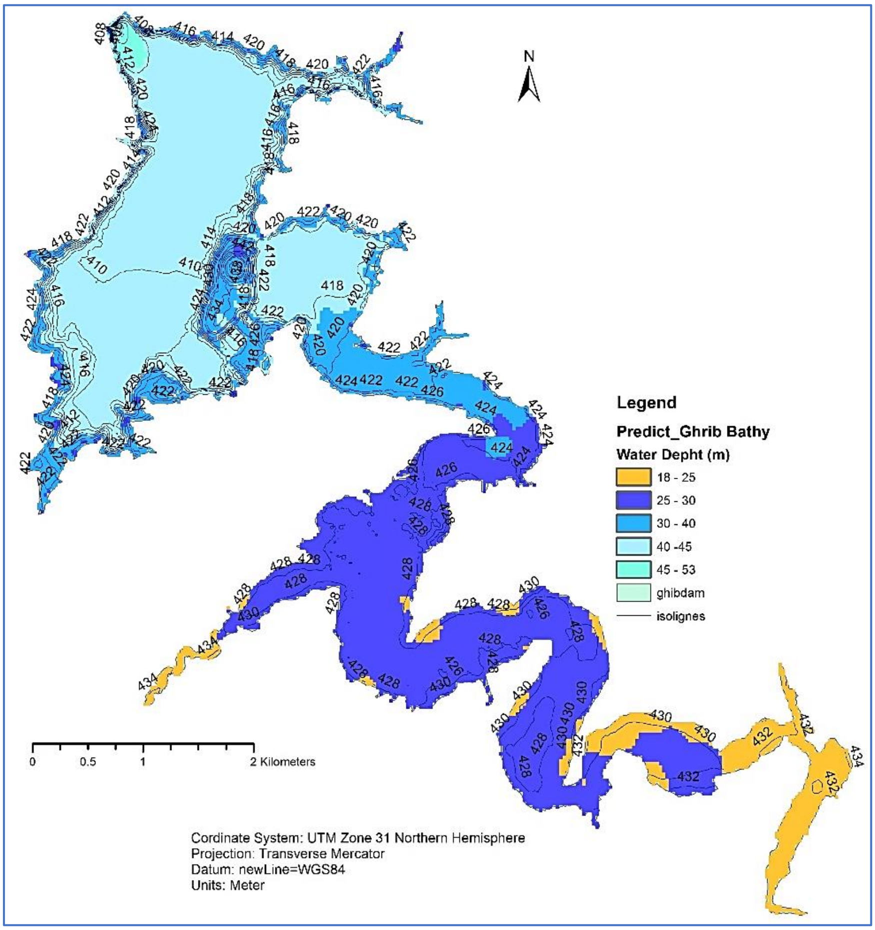

Fig. 17. Bathymetric Variation of the Ghrib dam.

This map displays the distribution of water depths in the Ghrib dam reservoir, divided into six classes. The minimum estimated water depth is approximately 18 meters, while the maximum reaches around 50 meters. Beyond this depth, up to about 105 meters, the areas are either solid land or sediment layers formed due to increased erosion and sediment transport in the region. These elevated values correspond to the outliers identified during the exploratory analysis phase.

This bathymetric map serves as a valuable tool for dam managers, providing detailed information on water depths across the entire Ghrib dam reservoir. However, predicting these depths solely from a raw bathymetric survey sample can be challenging. Therefore, it is recommended to use multiple survey samples and validate the map's accuracy through comprehensive comparisons and analyses.

5. CONCLUSIONS

This study focuses on the application of geostatistical methods integrated with geographic information systems (GIS) to predict bathymetric variations in the Ghrib Dam reservoir. A geostatistical analysis was conducted on a dataset comprising 44922 bathymetric survey points using the ordinary kriging interpolation technique. Four semivariogram fitting models were evaluated, and their performance was assessed through cross-validation. Based on the statistical parameters, the Gaussian model was selected to perform the interpolation operation. The resulting bathymetric map provides detailed insights into the water depth distribution across the Ghrib dam reservoir, revealing an average water depth of approximately 37 meters, with depths ranging from a minimum of around 18 meters to a maximum of about 53 meters. The generated bathymetric prediction map is a valuable tool for dam managers, enabling effective monitoring of water levels and sediment accumulation over time. It supports better management of dam operations, such as gate control and dredging activities. However, generating accurate bathymetric maps from raw survey data remains challenging due to numerous outliers. To improve accuracy, future studies could consider subdividing the dataset and conducting more focused geostatistical analyses. Although ordinary kriging has proven effective, it may be beneficial to explore alternative interpolation methods, such as universal kriging, spline interpolation, or inverse distance weighting (IDW), and compare their results to develop a more reliable and precise bathymetric map.

REFERENCES

AbdelRahman, MAE., Zakarya, Y.M., Metwaly, MM., Koubouris, G. (2021) Deciphering Soil Spatial Variability through Geostatistics and Interpolation Techniques. Sustainability 13(1),194, https://doi.org/10.3390/su13010194.

ABH, CZ. (2004) Agence du Bassin Hydrographique, Cheliff Zahrez, Cadastre hydraulique du bassin hydrographique du Cheliff- Aval du barrage de Boughzoul (*Hydraulic cadastre of the Cheliff hydrographic basin – Downstream of the Boughzoul dam*).

Adhikary, SK., Nitin Muttil, N., Yilmaz, AG. (2015) Genetic Programming-Based Ordinary Kriging for Spatial Interpolation of Rainfall. Journal of Hydrologic Engineering. Volume 21, Issue 2 https://doi.org/10.1061/(ASCE)HE.1943-5584.0001300

Adhikary, SK., Nitin Muttil, N., Gokhan Yilma, A. (2016) Ordinary kriging and genetic programming for spatial estimation of rainfall in the Middle Yarra River catchment, Australia. Hydrology Research 47 (6), 1182–1197, https://doi.org/10.2166/nh.2016.196

Alcaras, E., Parente, C., Vallario, A. (2020) Kriging interpolation of bathymetric data for 3D model of the Bay of Pozzuoli (Italy). IMEKO TC-19; International Workshop on Metrology for the Sea Naples, Italy, 5-7.

Alcaras, E., Amoroso, P., Parente, C. (2022) The Influence of Interpolated Point Location and Density on 3D Bathymetric Models Generated by Kriging Methods: An Application on the Giglio Island Seabed (Italy). Geosciences 12(2),62, https://doi.org/10.3390/geosciences12020062

ANBT. (2004) Rapport Technique, Barrage Ghrib wilaya de Ain Defla (*Technical Report, Ghrib Dam, Ain Defla Province*), p. 73.

ANBT. (2018) Agence nationale des barrages et transferts/1er Trimestre, Barrage du Ghrib (*National Agency for Dams and Transfers / 1st Quarter, Ghrib Dam*) pp. 36-40.

Arétouyap, Z., Njandjock Nouck, P., Nouayou, R., Ghomsi Kemgang, FE., Piépi Toko AD, Jamal Asfahani (2016) Lessening the adverse effect of the semivariogram model selection on an interpolative survey using kriging technique. *Springer Plus* 5, p. 549, https://doi.org/10.1186/s40064-016-2142-4

Arnaud, M., Emery, X. (2000) Estimation et interpolation de données spatiales méthodes déterministes et méthodes géostatistiques. Documents de travail de la Délégation Mathématiques et informatique appliquées N° 4-99, p. 230

Asadi, A., Adhikari, K.(2022) Minimizing Errors in the Prediction of Water Levels Using Kriging Technique in Residuals of the Groundwater Model. *Water 14*(3), p. 426, https://doi.org/10.3390/w14030426

Benallal, M. E. A., Abdelbaki C., Mourad, K.A., Badraoui, A., Kumar N. (2024) Assessing Water Demands and Allocation Strategies Using the Water Evaluation and Planning System—A Case Study of the Ghrib Basin, Algeria. Water 2024, 16 (19), 2832, https://doi.org/10.3390/w16192832

Benkaci, S. (2020) Impact du transport solide sur l'évolution des dépôts vaseux dans les barrages *(Impact of solid transport on the evolution of muddy deposits in dams)* Doctoral Thesis in Rural Engineering, Blida1 University, p. 169

Benkaci, S., Abir, D., Oumellal, A., Remini, B. (2018) Modélisation de l'érosion du bassin haut et moyen Cheliff par l'application Model builder sur ArcGis (Modeling the erosion of the upper and middle Cheliff basin by the Model builder application on ArcGis). Journal of Materials and Engineering Structures 5: 81–93 https://revue.ummto.dz/index.php/JMES/article/view/1676

Benkaci, S., Ghecham, S.E. (2021) Studying Sedimentation of the Ghrib dam using Model Builder ArcGIS Application. Recent Research on Hydrogeoly, Geoecologie and Atmospheric Sciences. Proceedings of the 1st MEDGU, Istanbul (Vol. 1), 51-54.

Biernacik, P., Kazimierski, W., Włodarczyk, S. (2023) Comparative Analysis of Selected Geostatistical Methods for Bottom Surface Modeling. *Sensors 23*(8): p. 3941, https://doi.org/10.3390/s23083941

Boubaker, Z., Bellatreche, M., Moussouni, A. (2010) Apport de la géostatistique à la prédiction de la diversité avienne dans le Parc National de Gouraya (Algérie) HAL open science. Rev. Écol. (Terre Vie), vol. 66, 215-229, doi: 10.3406/revec.2011.1594

Cardenas, G. (2004) Utilisation du module Geostatistical Analyst d'ARCVIEW dans le cadre de la qualité de l'air. Etude n°10 – INERIS DRC-04-55278-2IEN-GCa-04.0095, Rapport N° 3/3.

Chauvet, P. (1992) Traitement des données à support spatial : la géostatistique et ses usages. École Nationale Supérieure des Mines, Fontainebleau, p. 43

Desnoyers, Y. (2010) A methodological approach for the geostatistical characterization of radiological contaminations in nuclear facilities. Thesis for: PhD. p. 172, HAL Id: pastel-00839164 https://pastel.hal.science/pastel-00839164v1

Deutsch, CV. (2021) Implementation of Geostatistical Algorithms. *Math Geosci* 53, 227–237 https://doi.org/10.1007/s11004-020-09884-z

Endalew, L., Mulu, A. (2022) Comparison of the Sediment Yield Estimation Using Bathymetric Survey and Modified Universal Soil Loss Equation at Shumburit Reservoir, East Gojjam Zone Amhara Region, Ethiopia. Research Square, https://doi: 10.21203/rs.3.rs-2098547/v1.

ESRI. (2014) ArcMap version 10.2.2. User Manual. ESRI, 380 New York Street, Redlands, California, 92373-8100, USA. https://support.esri.com/en/download/ 2089.

Gharbia, A.S., Gharbia, S.S., Abushbak, T., Wafi, H., Aish A, Zelenakova M, Pilla F. (2016) Groundwater Quality Evaluation Using GIS Based Geostatistical Algorithms, Journal of Geoscience and Environment Protection: 89-103, http://www.scirp.org/journal/gep http://dx.doi.org/10.4236/gep.2016.42011

GIS Geography, (2023) How to Calculate Root Mean Square Error (RMSE) in Excel, Retrieved from: https://gisgeography.com/root-mean-square-error-rmse-gis/

GIS Geography, (2024) Kriging Interpolation – The Prediction Is Strong in this One, Retrieved from: https://gisgeography.com/kriging-interpolation-prediction/

Grekousis, G. (2020) Spatial Analysis Methods and Practice. Cambridge University Press, p. 532

Gundogdu, I.B. (2015) Geographically Weighted Regression and Secondary Variables for Mapping of Meteorological Data. Journal of Geodesy and Geomatics Engineering 2, pp. 63-72, doi: 10.17265/2332-8223/2015.06.001

Gupta, A., Kamble, T., Machiwal, D. (2017) Comparison of ordinary and Bayesian kriging techniques in depicting rainfall variability in arid and semi-arid regions of north-west India. Environ Earth Sci 76, p.512, https://doi.org/10.1007/s12665-017-6814-3

Hairan, M.H., Jamil, N.R., Azmai, M.N.AL., Looi, L.J., Aris, A.Z., Rosli, M.H. (2023) The Analysis of large dam impacts on sediment grain size distribution in a tropical river system. Civil Engineering Journal (E-ISSN: 2476-3055; P-ISSN: 2676-6957) Vol. 9, Special Issue, 15 "Innovative Strategies in Civil Engineering Grand Challenges" Doi: 10.28991/CEJ-SP2023-09-02

Hallouz, F., Meddi, M. (2022) A Sedimentary Investigation into the Origin and Composition of a Dam Reservoir. Book Flood Handbook 1st Edition- Imprint CRC Press, p. 24, eBook ISBN9780429463327

Isaaks, E.H., Srivastava, R.M. (1989) An Introduction to Applied Geostatistics. Oxford University Press: p. 413.

Ivan, H. (2021) Optimal interpolation method to predict the bathymetry of Saldanha Bay. Transactions in GIS 25(4),1649-2188, doi: 10.1111/tgis.12783

Johnston, K., Hoef, J.M., Krivoruchko, K., Luca, N. (2001) Using ArcGis Geostatistical Analyst. Esri Inc. Redlands, California, p. 306

Kelvin Kang, W.T., Mohd Razali, M. (2021) The Accuracy of Satellite Derived Bathymetry in Coastal and Shallow Water Zone. International Journal of Built Environment and Sustainability, Volume 8, Issue 3, Doi: https://doi.org/10.11113/ijbes.v8.n3.681

Khan, M.Z., Islam, M.R., Bin Abdus Salam, A., Ray, T. (2021) Spatial Variability and Geostatistical Analysis of Soil Properties in the Diversified Cropping Regions of Bangladesh Using Geographic Information System Techniques, Hindawi Applied and Environmental Soil Science, Article ID 6639180, p.19, https://doi.org/10.1155/2021/6639180

Khana, M., Almazah, M.M.A., EIlahi, A., Niaz, R., Al-Rezami, A.Y., Zaman, B. (2023) Spatial interpolation of water quality index based on Ordinary kriging and Universal kriging, Geomatics, Natural Hazards and Risk, DOI: 10.1080/19475705.2023.2190853

Le Blanc, M. (2006) Raising a silted reservoir as an alternative to dredging ; the example of Ghrib dam, Algeria. Hydroplus, France. Hydropower & dams, 2-4.

Makar, A. (2023) Coastal Bathymetric Sounding in Very Shallow Water Using USV: Study of Public Beach in Gdynia, Poland, *Sensors 23*(9), 4215, https://doi.org/10.3390/s23094215

Malherbe L., Rouïl, L. (2003) Méthodes de représentation de la qualité de l'air. Guide d'utilisation des méthodes de la géostatistique linéaire. INERIS DRC-03-45597-LRl-LMa –LCSQA-n°140_V1. p.70

Mälicke, M. (2022) SciKit-GStat 1.0: a SciPy-flavored geostatistical variogram estimation toolbox written in Python Geoscientific Model Development. GMD, Volume 15, issue 6: 2505–2532, https://doi.org/10.5194/gmd-15-2505-2022

Maliva, R.G. (2016) Geostatistical Methods and Applications. In: Aquifer Characterization Techniques. Springer Hydrogeology. Springer, Cham. https://doi.org/10.1007/978-3-319-32137-0_20

Mazzella, A. (2013) The Importance of the Model Choice for Experimental Semivariogram Modeling and Its Consequence in Evaluation Process. Journal of Engineering, Article ID 960105, p.10 https://doi.org/10.1155/2013/960105.

Mekonnen, Y.A., Mengistu, T.D., Asitatikie, A.N. (2022) Evaluation of reservoir sedimentation using bathymetry survey: a case study on Adebra night storage reservoir, Ethiopia. Appl Water Sci 12, p. 269 https://doi.org/10.1007/s13201-022-01787-0

Meylan, P. (1986) Régionalisation de données entachées d'erreurs de mesure par krigeage. Hydrologie Continentale, vol (1), 25-34.

Mokhtari, E., Farouk, M., Abdelkeb, B., Engel, B. (2023) Flood risk assessment using analytical hierarchy process: A case study from the Cheliff-Ghrib watershed, Algeria. J. *Water Clim. Chang.* , *14*, 694–711.

Pike, S., Traganos, D., Poursanidis, D., Williams, J., Medcalf, K., Reinartz, P., Chrysoulakis, N. (2019) Leveraging Commercial High Resolution Multispectral Satellite and Multibeam Sonar Data to Estimate Bathymetry: The Case Study of the Caribbean Sea. Remote Sens., 11, p. 1830 https://doi.org/10.3390/rs11151830

Qi, X., Wang, H., Pan, X., Chu J, Chiam, K. (2021) Prediction of interfaces of geological formations using the multivariate adaptive regression spline method. Underground Space Volume 6, Issue 3. pp. 252-266 https://doi.org/10.1016/j.undsp.2020.02.006

Rashid, I., Pandit, B. A. (2023) Various Remedial Measures for Dam Siltation. International Journal for Research in Applied Science & Engineering Technology (IJRASET) Volume 11 Issue XI, pp.486-488

Remini, B., Mokeddem, F.Z. (2018) Boukourdane (Algeria): a reservoir dam with low siltation rate, Larhyss Journal, ISSN 1112-3680, (n°35): pp. 29-44

Remini, B., Toumi, A. (2017) Le réservoir de Beni Haroun (Algérie) est-il menacé par l'envasement. LARHYSS Journal (ASJP)-Vol. 14, Iss, 29, pp. 249-263

Rigby, R.A., Stasinopoulos, M.D., Heller, G.Z., De Bastiani, F. (2019) Skewness and kurtosis comparisons of continuous distributions. In book: Distributions for Modeling Location, Scale, and Shape. 1st Edition, p. 18, doi: 10.1201/9780429298547-16

Rojimol, J., Phanindra, K.B.V.N., Umashankar, B. (2021) Application of Ordinary Kriging for In Situ Site Characterization. In: Patel, S., Solanki, C.H., Reddy, K.R., Shukla, S.K. (eds) Proceedings of the Indian Geotechnical Conference 2019. Lecture Notes in Civil Engineering, vol 137. Springer, Singapore, https://doi.org/10.1007/978-981-33-6466-0_51.

Saito, H., Mckenna, S.A, Zimmerman, D.A., Coburn, T.C. (2005) Geostatistical interpolation of object counts collected from multiple strip transects: ordinary kriging versus finite domain kriging. Stoch Environ Res Risk Assess. 19, pp. 71-85. DOI 10.1007/s00477-004-0207-3

Santra, P., Adhikary, P.P. (2021) Fundamentals of Geostatistics for Assessing Spatial Variation of Groundwater Resources. In: Adhikary, P.P., Shit, P.K., Santra, P., Bhunia, G.S., Tiwari, A.K., Chaudhary, B.S. (eds) Geostatistics and Geospatial Technologies for Groundwater Resources in India. Springer Hydrogeology. Springer, https://doi.org/10.1007/978-3-030-62397-5_1

Seddiki, A., Dehimi, S. (2023) Effect of choosing a variogram model to predict salinity and its impact on the environment and geotechnical structures. Technium Social Sciences Journal, 39 (1), 860–872 https://doi.org/10.47577/tssj.v39i1.8314

Selmy, S., Abd El-Aziz, S., El-Desoky, A., Moatez El-Sayed, M. (2022) Characterizing, predicting, and mapping of soil spatial variability in Gharb El-Mawhoub area of Dakhla Oasis using geostatistics and GIS approaches. Journal of the Saudi Society of Agricultural Sciences 21, pp. 383–396 https://doi.org/10.1016/j.jssas.2021.10.013

Šiljeg, A., Lozić, S., Šiljeg, S. (2015) A comparison of interpolation methods on the basis of data obtained from a bathymetric survey of Lake Vrana, Croatia, Hydrol. Earth Syst. Sci., 19, 3653–3666 https://doi.org/10.5194/hess-19-3653-2015

Šiljeg, A., Jurišić, M., Marić, I. (2016) Bathymetric measurement of Lake Skradinski buk, 23 septembre. Liste Geodetski (Hrvatsko geodetsko društvo) - Vol. 70, Iss : 3, pp. 231-252

Thomas, D. (2003) Analyse Spatiale avec ArcGis : méthodes et outils. Actes de la conférence francophone ESRI,

Tobgay, S. (2014) Temporal analysis of Area-Capacity curve for Hirakud reservoir, National institute of technology, Rourkela – 769008, p. 43

Triki, I., Hentati, I., Trabelsi, N., Zairi, M. (2014) Evaluation des techniques d'interpolation spatiale de la piézométrie à l'aide de l'extension Geostatistical Analyst d'ArcGis. Cas du système aquifère phréatique de Sfax (Tunisie). Géomatique Expert N°99, 55- 63

Varouchakis, E.A., Guardiola-Albert, C., Karatzas, G.P. (2022) Spatiotemporal geostatistical analysis of groundwater level in aquifer systems of complex hydrogeology. Water Resources Research, 58, e2021WR029988, https://doi.org/10.1029/2021WR029988

Wieskotten, M. (2023) Traitement géostatistique des résultats de mesure pour la caractérisation radiologique dans le cadre de l'assainissement /démantèlement de sites nucléaires. Université d'Avignon, Français. ffNNT: 2023AVIG0425ff : p.172, HAL Id: https://theses.hal.science/tel-04104483v1

Wilson, B., Singh, A., Sethi, A. (2022) Shallow Water Bathymetry Survey Using an Autonomous Surface Vehicle, IGARSS. IEEE International Geoscience and Remote Sensing Symposium, Kuala Lumpur, Malaysia: 7898-790, doi: 10.1109/IGARSS46834.2022.9884007

Wróbel, M., Mańk, K., Gawryś, R., Krysztofiak-Kaniewska, A., Boczoń, A., Grajewski, S. (2023) The use of low-cost bathymetric methods for the purpose of exploiting mid-forest water reservoirs. International Journal of Hydrology Science and Technology (IJHST), 16(1), 82-92. DOI: 10.1504/IJHST.2023.131835

Yoo, E.H. (2018) Geostatistical Approach to Spatial Data Transformation, In book: Reference Module in Earth Systems and Environmental Sciences. Comprehensive Geographic Information Systems: 253-263, DOI: 10.1016/B978-0-12-409548-9.09601-9

Zhu, R., Zheng, J., Zhang, J., Wang, H., Li, T., Liu, R. (2020) Application of the Sonar Detection Technique to Inspection of Vertical Quay Wall. J. Coast .Res. 95, 325–329 https://doi.org/10.2112/SI95-063.1